horticulturae

MDPI

Article

Seed Morphological Analysis in Species of *Vitis* and Relatives

José Javier Martín-Gómez [1], José Luis Rodríguez-Lorenzo [2], Diego Gutiérrez del Pozo [3], Félix Cabello Sáez de Santamaría [4], Gregorio Muñoz-Organero [4], Ángel Tocino [5] and Emilio Cervantes [1,*]

1 Instituto de Recursos Naturales y Agrobiología, Consejo Superior de Investigaciones Científicas, Cordel de Merinas 40, 37008 Salamanca, Spain
2 Plant Developmental Genetics, Institute of Biophysics v.v.i, Academy of Sciences of the Czech Republic, Královopolská 135, 612 65 Brno, Czech Republic
3 Herbario Amazónico del Ecuador ECUAMZ, Universidad Estatal Amazónica, Carretera Tena a Puyo Km. 44, Carlos Julio Arosemena Tola 150950, Ecuador
4 Finca El Encín, Instituto Madrileño de Investigación y Desarrollo Rural Agrario y Alimentario (IMIDRA), Autovía de Aragón Km, 38.2, Alcalá de Henares, 28800 Madrid, Spain
5 Departamento de Matemáticas, Facultad de Ciencias, Universidad de Salamanca, Plaza de la Merced 1-4, 37008 Salamanca, Spain
* Correspondence: emilio.cervantes@irnasa.csic.es

Abstract: Seed shape descriptions of species of *Vitis* have traditionally been based on adjectives comparing overall shape with geometric figures, such as oval, elongated oval, and pear-shaped, corresponding to higher values of the Stummer index (lower aspect ratio) for oval, and lower values of the Stummer index for pear shape (or elongated seeds, with a higher aspect ratio). Analytical, quantitative descriptions of shape have recently been applied to diverse genera of Vitaceae and cultivated varieties of *Vitis*. Here, we present the application of three quantitative methods to the seed shape description of ten species of the genus *Vitis* and three species of related genera (*Ampelopsis*, *Cissus* and *Parthenocissus*). First, general seed shape was described through comparisons using geometric models. For this, the average silhouettes of representative seed populations were used as models for shape quantification. Two additional quantitative methods were based on the measurement of bilateral symmetry and curvature analysis in the apex. Quantitative methods for shape description based on similarity with the models give an accurate account of the relationships between *Vitis* species. The resulting dendrogram is like the dendrogram obtained from a combined analysis using the data from general measurements and curvature and symmetry analyses. The original methods presented here for seed morphology are useful for analyzing the phylogenetic relationships between species of *Vitis*.

Keywords: curvature; models; polarity; symmetry

Citation: Martín-Gómez, J.J.; Rodríguez-Lorenzo, J.L.; Gutiérrez del Pozo, D.; Cabello Sáez de Santamaría, F.; Muñoz-Organero, G.; Tocino, Á.; Cervantes, E. Seed Morphological Analysis in Species of *Vitis* and Relatives. *Horticulturae* **2024**, *10*, 285. https://doi.org/10.3390/horticulturae10030285

Academic Editor: Sergio Ruffo Roberto

Received: 19 February 2024
Revised: 4 March 2024
Accepted: 8 March 2024
Published: 16 March 2024

1. Introduction

Grapevines are economically important fruit crops produced from hundreds of varieties traditionally cultured worldwide and belonging to the genus *Vitis* L. (Vitaceae Juss.), which comprises eighty-one species of climbers and shrubs of wide distribution in America, Africa, Asia and Europe [1–5]. Although the European varieties of *Vitis vinifera* L. were traditionally considered to proceed from the domestication of *V. vinifera* subsp. (or var.) *sylvestris*, recent work presents a more complex panorama, with most of the wild European specimens of grapevines belonging to a complex group of foreign invader taxa, including true and hybrid species of *V. riparia* Michx., *V. rupestris* Scheele, *V. berlandieri* Planch. and others [6–8], whose rootstocks, mostly coming from North America, were used as graftstock to defend the European grapevine against the phylloxera disease that invaded European cultures in the late decades of the 19th century [6–8].

The morphological description of *Vitis* seeds may contribute to the taxonomy of species in this genus, as well as to the description of its varieties. As for other plant species, seed

morphology has relied traditionally on diverse measurements as well as on the qualitative appreciation of overall seed shape based on adjectives reflecting similarity with geometric forms, such as cordate, globose, oval, pear-shaped, rounded, squat or triangular [9–16], assuming generally smaller and more rounded seeds in wild specimens and more elongated, pear-shaped seeds in cultivated varieties [17]. Quantitative analytical methods include those based on the Fourier transform [18–23], and also the direct comparison with reference images, and to this end, a series of geometric models have been applied for the seeds in the Vitaceae [24,25], and more specific models have been adjusted to define seed shape in varieties of *Vitis* representative of the biodiversity in the Spanish germplasm collection stored at the Instituto Madrileño de Investigación Agraria y Desarrollo Rural, Agrario y Alimentario (IMIDRA), Finca "El Encin", Alcalá de Henares, Madrid [25].

In addition to overall seed shape description, other quantitative aspects in the analysis of seed morphology comprise the measurement of symmetry and curvature in the apex. Both aspects have been recently applied to seeds of representative species of the Cucurbitaceae [26]. The curvature of a plane curve is a magnitude that measures the rate at which the tangent line turns per unit distance moved along the curve. To determine curvature in the curve formed by the image of a natural organ, such as the root or the seed apex, first, Bézier curves are obtained, representing the corresponding silhouettes. Curvature was measured in the root apex of *Arabidopsis* Heinh. (Brassicaceae), showing reduced values in ethylene-insensitive mutants (*etr1-1* and *ein2-1*) [27], as well as under hydrogen peroxide treatment [28]. In addition, curvature analysis allowed for the differentiation of morphotypes in wheat kernels [29] and the definition of three groups of seeds in cultivated grapevine varieties, depending on the shape of the seed apex [30]. While in most cultivars, the seed apex is plane, others have an acute seed apex, with a single maximum of curvature, or intermediate types. The variation found in curvature types, together with the similarity to models, may contribute to the establishment of relationships in the taxonomy of *Vitis*. Increases in the sizes of berries and seeds, a consequence of the process of domestication, are accompanied by increased carbohydrate accumulation, cuticle deposition and seed thickening, resulting in a broader seed apex. The original methods reported here for seed morphological analysis can be an interesting complement in the description, identification, and classification of the species of the genus in the study of phylogenetic relationships between the species and varieties of *Vitis*, which are currently being investigated via molecular analysis.

2. Materials and Methods

2.1. Seeds of Vitis Species and Relatives

Table 1 presents a list of the species analyzed in this work. These include *Ampelopsis aconitifolia* Bunge, *Cissus verticillata* (L.) Nicolson and C.E. Jarvis, *Parthenocissus quinquefolia* (L.) Planch, nine species of *Vitis* L. and the hybrid *Vitis* x *doaniana* Munson ex Viala, resulting from the cross *V. acerifolia* × *V. mustangensis* [5]. Seeds were obtained from plants grown at IMIDRA, except for *Cissus verticillata*. Seeds of *C. verticillata* were collected at Pastaza (Ecuador) in disturbed areas and, after being photographed, the seeds were returned to the wild.

2.2. Photography

Photographs were captured using a Sony ILCE 5100 digital camera equipped with an AF-S Micro NIKKOR 60 mm 1:2.8 G ED objective (Nikon, Tokio, Japan). They were organized in groups of 20 seeds per species as JPEG images (300 ppp). Color photographs were converted to grayscale silhouettes and kept as images of 20 seeds per species for the analyses of general morphological characters and symmetry, and comparison with models. Both the seed images and silhouettes are available in Zenodo (See Supplementary Materials).

Table 1. Species analyzed in this work. Tribes are major clades in the Vitaceae as recognized in [31].

Species	Tribe
Ampelopsis aconitifolia Bunge	Ampelopsideae
Cissus verticillata (L.) Nicolson and C.E. Jarvis	Cisseae
Parthenocissus quinquefolia (L.) Planch.	Parthenocisseae
Vitis aestivalis Michx.	Viteae
Vitis amurensis Rupr.	Viteae
Vitis berlandieri Planch.	Viteae
Vitis californica Parry	Viteae
Vitis candicans Engelm. ex A.Gray	Viteae
Vitis x *doaniana* Munson ex Viala	Viteae
Vitis labrusca L.	Viteae
Vitis riparia A. Gray	Viteae
Vitis rupestris Scheele	Viteae

2.3. General Morphological Descriptors

Photographs were used to derive data on seed area (A), perimeter (P), length of the major axis (L), length of the minor axis (W), aspect ratio (AR is the ratio L/W), circularity (C), roundness (R), and solidity (S). These measurements were conducted using the Image J program (version v1.8.0) [32]. The seeds were vertically oriented, with length and width corresponding, respectively, with the vertical and horizontal Feret diameters. Feret, or caliper diameters, are the distances between two parallel planes restricting the object. The circularity index and roundness were calculated as described [33–35].

2.4. Average Silhouettes for Each Species

Average silhouettes represent the typical shape of each set of 20 silhouettes of every species. The protocol used to extract average silhouettes from a set of images has been described by Cervantes et al. [25] (See Supplementary Materials). Average silhouettes were used as models for comparisons with images of all species. Models were denoted with the initial "M" followed by the first four letters corresponding to genera or species such as Maest, Mamur, Mberl, etc., for *Vitis* species and MAmpe, MCiss, and MPart for the models corresponding to *Ampelopsis aconitifolia*, *Cissus verticillata* and *Parthenocissus quinquefolia*, respectively.

2.5. Quantification of Seed Shape by the J Index

Average silhouettes were used as models for shape quantification. For this purpose, the average silhouette for each species was compared to 20 seed silhouettes of all species.

The *J* index was calculated as the percentage of similarity between each seed image and the corresponding model. To perform this calculation, the model was superimposed upon the seed image, and two copies of the combined image were created: one with the model in white and the other with the model in black (Figure 1). The areas of both regions were quantified with Image J. The area with the model in black is the total area, and the area with the model in white is the area shared between each image and the model. *J* index is the percent of similarity between the seed image and the model and is calculated as follows:

$$J \text{ index} = \frac{\text{Shared area}}{\text{Total area}} \times 100$$

The images used for *J* index calculations are available at Zenodo (See Supplementary Materials).

2.6. Symmetry Analysis

Similar to the calculation of *J* index, the quantification of bilateral symmetry involved comparing two images. In this case, the model used was the silhouette of the horizontal reflection of each seed. The images used for symmetry calculations are available at Zenodo (See Supplementary Materials).

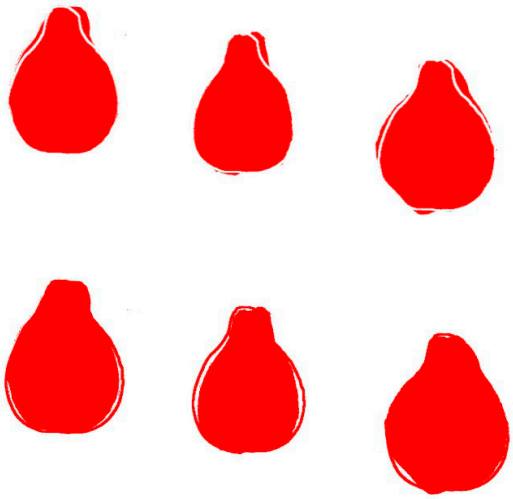

Figure 1. Figures resulting from the superposition of models to seed images and treatment with Image J. In the three seeds above, the models are stored in white, and only the common region between seed and model is measured (shared area), while in the seed images below, the models are stored in black (red after thresholding), thus the area measured is the sum of the area occupied by the seed and that occupied by the model (Total area). The image corresponds to three seeds of *V. aestivalis* with the average silhouette of this species. *J* indices for these seeds are 90.0, 88.1 and 88.3, respectively.

2.7. Curvature Analysis

Maximum and mean curvature values, along with the ratio between maximum and mean curvature, were determined for the apical side of seeds for each species following established procedures [27–30] (see Supplementary Materials). Curvature measurements were conducted automatically with the function Analyze line graph of Image J. Between 20 and 25 representative seeds were analyzed for each species. Vertically oriented images (JPEG) were opened in Image J and converted to 8-bit, and threshold values were then adjusted. The curve corresponding to the seed apex was selected from the outlines, and a new threshold was defined before the corresponding line graph was analyzed to give the x and y coordinates. The coordinates served as the basis for calculating the Bézier curves and the corresponding curvature values in Mathematica according to published protocols [27–30]. Curvature was given in micron^{-1} $\times$ 1000; thus, a curvature of 20 corresponds to a circumference of 50 microns (1/50 $\times$ 1000) and a curvature of 2 corresponds to a circumference of 0.5 mm. A quotient from the maximum and mean curvatures close to 1 indicates a curve approaching the arc of a circumference with radius equal to the inverse of mean curvature value.

2.8. Statistical Analysis

Due to heterogeneity in sample sizes or in their distributions, Kruskal Wallis test was used to analyze differences between populations for the measurements. Statistical analyses were conducted with IBM SPSS statistics v28 (SPSS 2021). Coefficients of variation were calculated according to [36].

3. Results

3.1. General Morphological Measurements

Table 2 contains a summary of the mean values for area (A), perimeter (P), length (L), width (W), circularity (C), aspect ratio (AR), roundness (R) and solidity (S) for seeds of the species analyzed. There were significant differences in all measurements and, as reported in the analysis of seed shape in other plant families [37], the lowest coefficients of variation were found in solidity. With the exceptions of *V. amurensis*, *V. californica*, and *V.*

rupestris, the species of *Vitis* were larger than those of the other three genera. The lowest values of size measurements (A, P, L, W) corresponded to *Ampelopsis aconitifolia*, followed by *Cissus verticillata*. The largest size was found for *V. labrusca*, followed by *V. doaniana*. The lowest circularity was observed in *C. verticillata* and *V. aestivalis*, followed by a second group including *V. labrusca* and *V. riparia*. The aspect ratio varied between 1.14 (*Parthenocisus quinquefolia*) and 1.69 (*Vitis aestivalis*). Among *Vitis* species, *V. amurensis*, *V. californica*, *V. candicans*, *V. doaniana*, *V. labrusca* and *V. rupestris* had similar aspect ratio values between 1.29 and 1.35. The values of aspect ratio are inverse to those of the Stummer index, a traditional measurement used in Viticulture. For the *Vitis* species used in this study, the Stummer index is indicated in the footer of Table 2. Significant differences were found in the variable solidity with the highest values corresponding to the group formed by *Parthenocisus quinquefolia*, *V. californica*, and *V. candicans*, whereas the lowest value was found for *V. labrusca*.

Table 2. Results of the comparison (Kruskal–Wallis test) of general morphological measurements, indicating the mean values (coefficients of variation between parentheses) for area (A), perimeter (P), length (L), width (W), circularity (C), aspect ratio (AR), roundness (R) and solidity (S) of the seed images for 10 species of *Vitis* and three related species. P, L and W are given in mm; A is given in mm^2. Different super index letters indicate significant differences between numbers in each column.

Species	A	P	L	W	C	AR	R	S
Ampelopsis aconitifolia Bunge	9.71 ^{a} (6.4)	12.37 ^{a} (4.4)	3.90 ^{a} (4.1)	3.17 ^{a} (3.7)	0.80 ^{efg} (4.0)	1.23 ^{b} (4.5)	0.81 ^{e} (4.5)	0.975 ^{e} (0.8)
Cissus verticillata (L.) Nicolson and C.E. Jarvis	11.65 ^{b} (5.5)	14.44 ^{b} (3.6)	4.55 ^{b} (3.1)	3.26 ^{b} (3.1)	0.70 ^{a} (5.5)	1.40 ^{d} (2.8)	0.72 ^{c} (2.7)	0.957 ^{b} (0.6)
Parthenocisus quinquefolia (L.) Planch.	14.84 ^{d} (6.3)	15.24 ^{c} (3.2)	4.64 ^{b} (4.9)	4.07 ^{f} (5.0)	0.80 ^{fg} (2.8)	1.14 ^{a} (7.6)	0.88 ^{f} (7.6)	0.982 ^{f} (0.4)
Vitis aestivalis Michx.	17.92 ^{f} (8.5)	17.87 ^{f} (4.3)	6.21 ^{gh} (6.0)	3.68 ^{c} (6.4)	0.70 ^{a} (4.1)	1.69 ^{f} (9.4)	0.60 ^{a} (9.8)	0.961 ^{bc} (1.62)
Vitis amurensis Rupr.	13.95 ^{c} (4.90)	14.73 ^{b} (3.0)	4.85 ^{c} (3.3)	3.66 ^{c} (3.4)	0.81 ^{g} (2.6)	1.32 ^{c} (4.4)	0.76 ^{d} (4.4)	0.973 ^{de} (0.42)
Vitis berlandieri Planch.	17.40 ^{ef} (5.2)	15.95 ^{e} (3.0)	5.70 ^{e} (4.2)	3.89 ^{de} (4.7)	0.76 ^{c} (3.0)	1.47 ^{e} (7.2)	0.68 ^{b} (7.2)	0.971 ^{d} (0.5)
Vitis californica Parry	14.67 ^{cd} (10.0)	15.19 ^{c} (5.5)	4.99 ^{c} (7.7)	3.75 ^{cd} (7.7)	0.80 ^{defg} (3.7)	1.34 ^{c} (12.1)	0.76 ^{de} (11.7)	0.981 ^{f} (0.5)
Vitis candicans Engelm. ex A.Gray	16.85 ^{e} (7.9)	16.62 ^{de} (4.4)	5.26 ^{d} (4.2)	4.08 ^{ef} (7.1)	0.77 ^{cd} (7.1)	1.30 ^{bc} (8.9)	0.78 ^{def} (8.7)	0.981 ^{f} (0.46)
Vitis doaniana Munson ex Viala	22.21 ^{h} (5.3)	18.46 ^{g} (2.5)	5.96 ^{f} (3.4)	4.54 ^{g} (4.3)	0.78 ^{cdef} (2.7)	1.32 ^{c} (5.8)	0.76 ^{d} (5.6)	0.975 ^{e} (0.4)
Vitis labrusca L.	23.81 ^{i} (6.6)	20.25 ^{h} (5.1)	6.39 ^{h} (5.0)	4.75 ^{h} (3.9)	0.73 ^{b} (5.9)	1.35 ^{c} (5.9)	0.75 ^{d} (5.9)	0.949 ^{a} (1.4)
Vitis riparia A. Gray	19.35 ^{g} (7.4)	18.09 ^{f} (3.8)	6.07 ^{fg} (4.5)	4.06 ^{f} (5.0)	0.74 ^{b} (3.4)	1.50 ^{e} (6.1)	0.67 ^{b} (6.1)	0.963 ^{c} (0.8)
Vitis rupestris Scheele	15.62 ^{d} (13.8)	15.90 ^{cd} (7.7)	5.05 ^{c} (9.0)	3.93 ^{def} (6.0)	0.77 ^{cde} (3.8)	1.29 ^{bc} (6.4)	0.78 ^{de} (6.2)	0.965 ^{c} (0.9)

Values of aspect ratio are inverse to those of Stummer index (SI). The SI for 9 species of *Vitis* was as follows: *V. aestivalis*, 0.59; *V. amurensis*, 0.76; *V. berlandieri*, 0.68; *V. californica*, 0.75; *V. candicans*, 0.77; *V. doaniana*, 0.76; *V. labrusca*, 0.74; *V. riparia*, 0.67; *V. rupestris*, 0.78.

3.2. Average Silhouettes of Representative Species

Figure 2 shows the average silhouettes for each species. A total of twelve average silhouettes were compared with 20 seeds representative of each species.

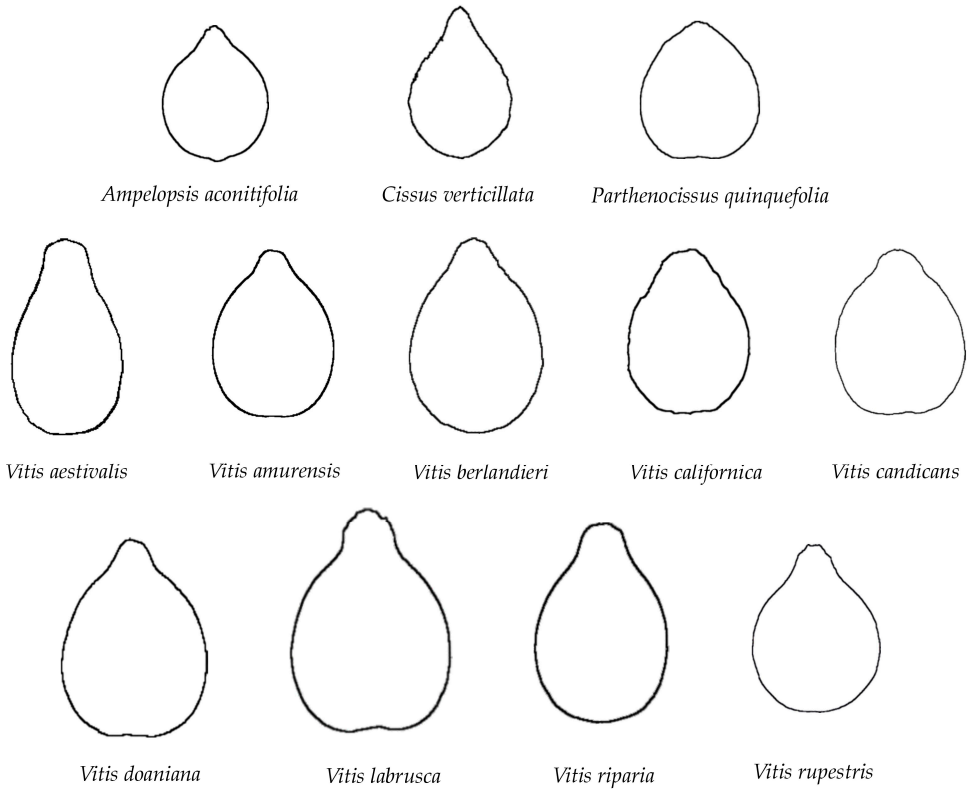

Figure 2. Average seed silhouettes of species analyzed. Bar represents 1 cm.

3.3. Comparison of Seed Shape between Species by the J *Index*

The average silhouette for each species was used to calculate the mean *J* index values against the 20 seed images of each species, and the results are shown in Table 3. Despite all models showing the highest value for the species, some models display maximum values for other species. In the case of the model derived from the average silhouette of *V. californica*, maximum values resulted from all the combinations except for that with *V. aestivalis*. This is the result of a large variation in seed shape in this species. The difference between the value given by a model for its own species and the value for another species indicates species-specific shape, and this was remarkable in *A. aconitifolia*, *C. verticillata*, *P. quinquefolia*, *V. aestivalis*, and *V. riparia*. This difference did not appear in the other species. In particular, the models of *V. berlandieri*, *V. californica*, *V. candicans*, *V. doaniana* and *V. rupestris* gave relatively high values of *J* index with different species. The dendrogram resulting from the comparisons is shown in Figure 3. A similar dendrogram resulted from the combined analysis with data resulting from general measurements, as well as curvature and symmetry analyses.

The dendrogram in Figure 3 shows the hierarchical relationship between species. The species of *Vitis* are categorized into two main groups, with five and three species, respectively. The position of *V. aestivalis* outside of these two groups requires further confirmation. In the major group, *V. riparia* and *V. berlandieri* appear closely related, while *V. amurensis* and *V. doaniana* are close together in another branch.

Table 3. Results of the comparison (Kruskal–Wallis test) of *J* index values in the seed images of different species with average silhouettes as models (coefficients of variation between parentheses). Different super index letters indicate significant differences between numbers in each column. Detached in bold are the values corresponding to seeds of a given species with their average silhouette included as the model. Abbreviations refer to the average silhouette of each species.

Species	Model											
	MAac	**MCve**	**MPqu**	**MVae**	**MVam**	**MVbe**	**MVca**	**MVcan**	**MVdo**	**MVla**	**MVri**	**MVru**
A. aconitifolia	**90.0** ^{f} (1.6)	83.9 ^{abc} (3.2)	88.7 ^{e} (1.9)	73.2 ^{b} (4.3)	88.5 ^{cdef} (2.8)	86.5 ^{bcd} (2.7)	87.3 ^{cde} (1.5)	90.9 ^{e} (1.7)	89.1 ^{cd} (2.2)	84.6 ^{bc} (3.3)	81.7 ^{b} (3.8)	90.4 ^{e} (1.7)
C. verticillata	86.1 ^{cd} (1.8)	**89.3** ^{g} (0.9)	82.1 ^{c} (2.0)	80.1 ^{d} (2.0)	89.3 ^{ef} (1.3)	89.8 ^{fg} (1.2)	87.9 ^{de} (0.9)	89.1 ^{c} (1.1)	89.6 ^{d} (1.2)	88.6 ^{f} (1.0)	87.6 ^{f} (1.0)	90.0 ^{e} (1.6)
P. quinquefolia	87.5 ^{de} (2.4)	80.5 ^{a} (5.6)	**90.2** ^{f} (1.9)	66.6 ^{a} (5.2)	84.2 ^{ab} (5.5)	79.2 ^{a} (6.3)	83.6 ^{b} (4.7)	88.6 ^{cde} (4.6)	85.7 ^{b} (4.9)	81.6 ^{a} (4.4)	77.7 ^{a} (5.6)	85.2 ^{b} (3.9)
V. aestivalis	76.9 ^{a} (6.2)	83.5 ^{abc} (3.8)	71.7 ^{a} (6.7)	**87.5** ^{f} (4.3)	81.8 ^{a} (5.6)	84.0 ^{b} (4.8)	80.6 ^{a} (5.3)	79.9 ^{a} (6.0)	81.6 ^{a} (5.3)	83.1 ^{ab} (4.7)	84.9 ^{cde} (3.8)	81.0 ^{a} (5.2)
V. amurensis	87.8 ^{e} (2.1)	87.1 ^{f} (1.2)	85.4 ^{d} (2.8)	77.1 ^{c} (2.9)	**91.1** ^{g} (1.1)	89.3 ^{efg} (2.1)	88.3 ^{e} (1.0)	91.2 ^{e} (1.7)	91.2 ^{e} (1.0)	87.9 ^{ef} (1.8)	86.1 ^{de} (1.8)	90.3 ^{e} (1.1)
V. berlandieri	84.8 ^{c} (3.8)	86.3 ^{def} (1.6)	80.4 ^{bc} (5.0)	81.9 ^{d} (4.4)	89.0 ^{ef} (3.1)	**89.9** ^{g} (2.5)	86.9 ^{cde} (3.0)	87.9 ^{bc} (3.7)	88.4 ^{cd} (3.6)	86.3 ^{cde} (2.6)	87.0 ^{ef} (1.9)	86.9 ^{bcd} (3.6)
V. californica	86.4 ^{cde} (4.0)	82.6 ^{ab} (4.0)	85.6 ^{de} (6.5)	75.6 ^{bc} (8.3)	86.7 ^{bc} (2.5)	85.7 ^{bcd} (4.1)	**86.5** ^{bcde} (3.3)	88.8 ^{cde} (3.9)	86.9 ^{b} (2.4)	84.4 ^{b} (2.7)	81.8 ^{bc} (6.1)	86.4 ^{bc} (2.9)
V. candicans	87.9 ^{e} (2.3)	84.4 ^{bcd} (2.6)	87.0 ^{de} (4.1)	75.6 ^{bc} (5.2)	89.0 ^{def} (2.6)	86.1 ^{bcde} (4.6)	87.4 ^{de} (2.0)	**91.4** ^{e} (2.0)	89.0 ^{cd} (2.0)	85.6 ^{bcd} (2.7)	83.2 ^{bcd} (4.1)	88.8 ^{d} (1.7)
V. doaniana	87.9 ^{e} (2.2)	86.4 ^{ef} (2.7)	85.3 ^{d} (3.6)	77.2 ^{c} (4.3)	90.4 ^{fg} (1.8)	87.8 ^{cdef} (2.9)	87.7 ^{de} (1.7)	90.9 ^{e} (1.8)	**90.7** ^{e} (2.0)	87.5 ^{def} (2.3)	84.8 ^{cd} (3.0)	90.0 ^{e} (2.0)
V. labrusca	85.0 ^{c} (3.2)	85.4 ^{cde} (2.2)	81.9 ^{c} (4.4)	77.9 ^{c} (3.1)	87.4 ^{cde} (3.3)	85.3 ^{bc} (3.1)	85.3 ^{bc} (2.9)	88.9 ^{cd} (2.6)	88.7 ^{cd} (2.6)	**88.6** ^{f} (2.1)	83.6 ^{bc} (2.7)	87.9 ^{cd} (3.1)
V. riparia	82.5 ^{b} (3.2)	87.3 ^{f} (1.6)	78.0 ^{b} (3.5)	84.5 ^{e} (3.4)	87.5 ^{cd} (2.7)	89.3 ^{fg} (1.8)	86.2 ^{bcd} (2.0)	86.4 ^{b} (3.0)	87.3 ^{bc} (2.5)	86.9 ^{de} (2.2)	**88.1** ^{g} (1.6)	85.9 ^{b} (2.9)
V. rupestris	88.3 ^{e} (2.4)	86.8 ^{ef} (2.6)	87.3 ^{de} (2.0)	77.2 ^{c} (3.7)	89.3 ^{ef} (1.3)	88.3 ^{def} (2.4)	87.7 ^{de} (1.4)	90.8 ^{de} (1.3)	90.3 ^{de} (1.1)	87.8 ^{ef} (2.2)	85.0 ^{cd} (3.3)	**90.9** ^{e} (1.4)

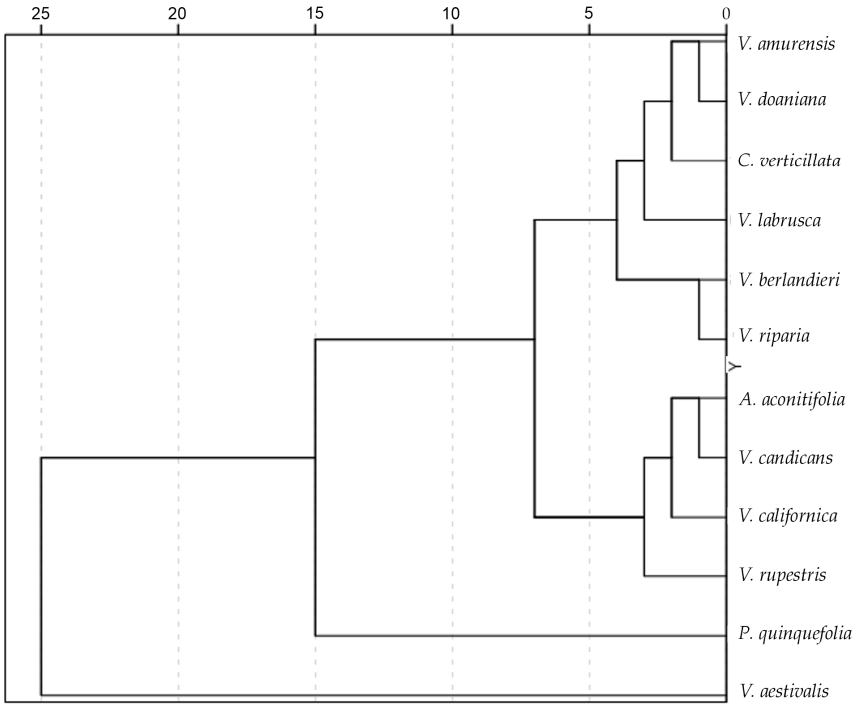

Figure 3. Dendrogram showing the relationship between species analyzed based on their similarity with the models from average silhouettes of each species.

3.4. Curvature Analysis

3.4.1. Curvature Measurements

Table 4 presents the maximum and mean curvature values and maximum to mean rate for 12 species. The maximum curvature was between 2.16 and 5.07 and distributed in the species forming five groups with significant differences between them. The highest values were observed in *Ampelopsis aconitifolia*, *Cissus verticillata* and *V. berlandieri*, followed by *V. amurensis* and *V. doaniana*; a third group included *Parthenocissus quinquefolia*, *V. labrusca* and *V. rupestris*. Intermediate low values were found for *V. aestivalis*, and the lowest values were found in *V. californica*. *V. candicans* had values between those of *V. aestivalis* and *V. riparia*, and this species had values close to that of *P. quinquefolia.* Mean curvature values were between 0.35 (*V. labrusca*) and 0.65 (*Cissus verticillata*), and split the species into five groups, with some intermediate values between them. The highest mean curvature corresponded to *Ampelopsis aconitifolia* and *Cissus verticillata*, followed by *V. aestivalis*. A third group was formed by *V. berlandieri* and *V. doaniana*, followed by *V. riparia*, and finally the lowest mean curvature values corresponded to *V. labrusca*. Ratio max. to mean curvature values were between 4.57 (*V. californica*) and 10.08 (*V. berlandieri*), indicating that the mean curvature values were considerably lower than the maximum values.

Table 4. Results of the comparison (Kruskal–Wallis test) of curvature in the seed apex, indicating the mean values (coefficients of variation between parentheses) for maximum curvature (Max C.), mean curvature (Mean C.) and Max to mean curvature ratio (Ratio) for 10 species of *Vitis* and 3 related species. Different super index letters indicate significant differences between means for the same measurement (same column). N is the number of seeds analyzed. Curvature values are given in mm^{-1}.

Species	N	Max C.	Mean C.	Ratio
Ampelopsis aconitifolia Bunge	20	5.07 ^{f} (22.87)	0.59 ^{g} (4.58)	8.60 ^{def} (25.05)
Cissus verticillata Nicolson and C.E. Jarvis	20	5.03 ^{f} (26.65)	0.65 ^{g} (30.73)	10.0 ^{ef} (25.26)
Parthenocisus quinquefolia (L.) Planch.	21	3.08 ^{d} (15.87)	0.47 ^{de} (14.66)	6.56 ^{c} (12.73)
Vitis aestivalis Michx.	18	2.53 ^{b} (17.92)	0.64 ^{f} (57.89)	4.98 ^{b} (57.81)
Vitis amurensis Rupr.	20	4.15 ^{e} (14.31)	0.52 ^{ef} (5.38)	7.94 ^{de} (12.91)
Vitis berlandieri Planch.	10	4.79 ^{f} (8.72)	0.48 ^{d} (3.25)	10.08 ^{f} (10.63)
Vitis californica Parry	20	2.16 ^{a} (66.69)	0.50 ^{def} (17.75)	4.57 ^{a} (91.66)
Vitis candicans Engelm. ex A.Gray	20	2.54 ^{bc} (19.13)	0.37 ^{ab} (11.03)	6.91 ^{c} (19.31)
Vitis doaniana Munson ex Viala	19	4.13 ^{e} (14.43)	0.48 ^{d} (11.00)	8.74 ^{ef} (17.32)
Vitis labrusca L.	19	3.39 ^{d} (41.78)	0.35 ^{a} (15.70)	9.91 ^{ef} (45.46)
Vitis riparia A. Gray	22	3.12 ^{cd} (38.34)	0.44 ^{c} (12.85)	7.03 ^{cd} (34.27)
Vitis rupestris Scheele	22	3.30 ^{d} (21.17)	0.40 ^{b} (15.15)	8.39 ^{def} (22.97)

3.4.2. Seed Morphological Analysis

Depending on the shape of the apex, the seeds were divided into three groups: seeds with one point of maximum curvature (acute), seeds with two peaks (plane) and seeds of a mixed type with one or two peaks, variable among the seeds. The first group (see Section 1) includes *A. aconitifolia*, *C. verticillata*, *P. quinquefolia* and three species of *Vitis*: *V. amurensis*, *V. doaniana*, and *V. labrusca*. The second group (see Section 2) is composed of four species of *Vitis*: *V. aestivalis*, *V. berlandieri*, *V. candicans* and *V. rupestris*. The group of species with mixed types of seed peaks includes *V. californica* and *V. riparia;* see Section 3. The following sub-sections contain images with a representative example of each of these three types. The remaining are given in Appendix A.

Section 1: Genera and Species with One Point of Maximum Curvature at Their Seed Apex (Acute)

Figure 4 shows the images of four seeds of *A. aconitifolia* with the Bézier curves representing their apex and the corresponding curvature values. Similar figures were obtained for the other species in this group (Figures A1–A5 in Appendix A).

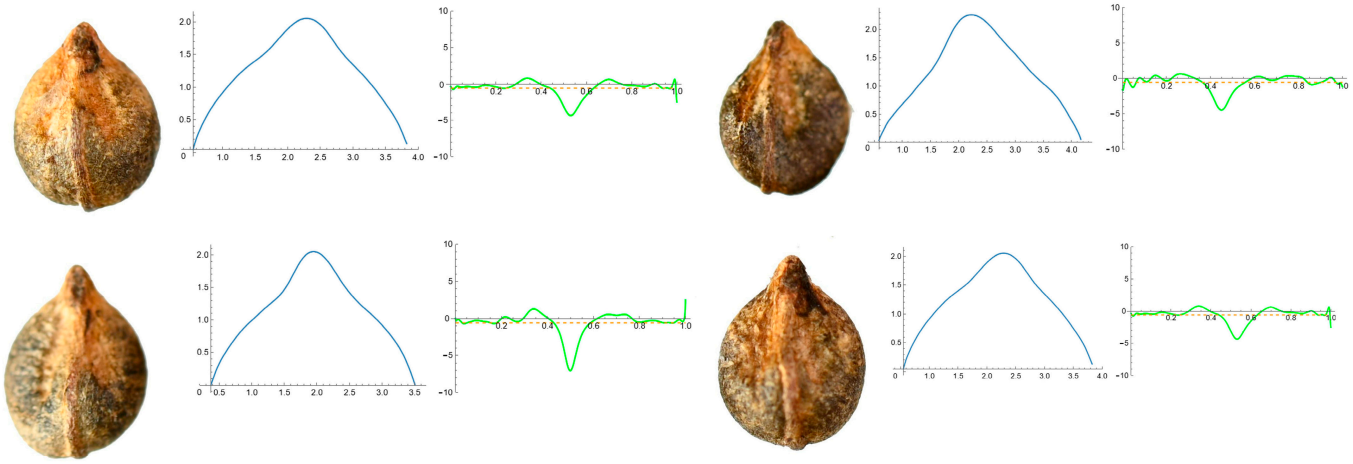

Figure 4. Four representative seeds of *Ampelopsis aconitifolia* with their respective Bézier curves representing their apex and the corresponding curvature values. Bar represents 5 mm. Solid lines in blue: Bézier curve. Solid lines in green: curvature. Dashed lines: mean curvature.

Section 2: Species with Two Points of Maximum Curvature at Their Apex (Plane)

This group is composed of *V. aestivalis*, *V. berlandieri*, *V. candicans* and *V. rupestris*. Seed images, Bézier curves and curvature values for *V. aestivalis* are shown in Figure 5, and for the other three species they are shown in Figures A6–A8 in Appendix A.

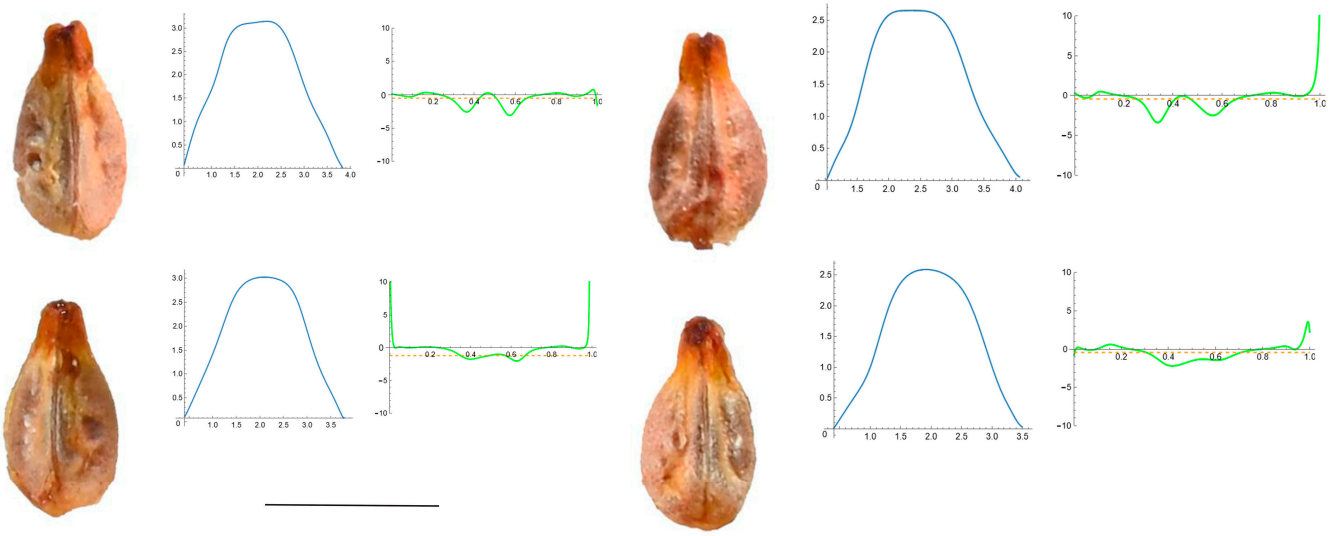

Figure 5. Four representative seeds of *Vitis aestivalis* with their respective Bézier curves representing their apex and the corresponding curvature values. Bar represents 5 mm. Solid lines in blue: Bézier curve. Solid lines in green: curvature. Dashed lines: mean curvature.

Section 3: Species of an Intermediate or Mixed Type at Their Apex (Acute and Plane)

The intermediate-type seeds included those of *V. californica* and *V. riparia*, as shown in Figures 6 and 7, respectively.

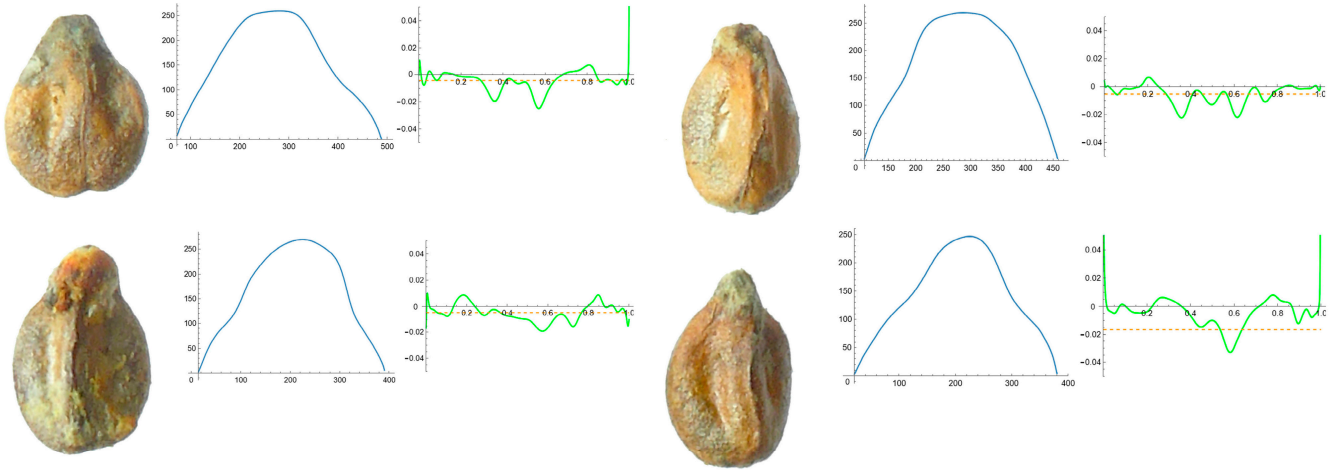

Figure 6. Four representative seeds of *Vitis californica* with their respective Bézier curves representing their apex and the corresponding curvature values. Bar represents 5 mm. Solid lines in blue: Bézier curve. Solid lines in green: curvature. Dashed lines: mean curvature.

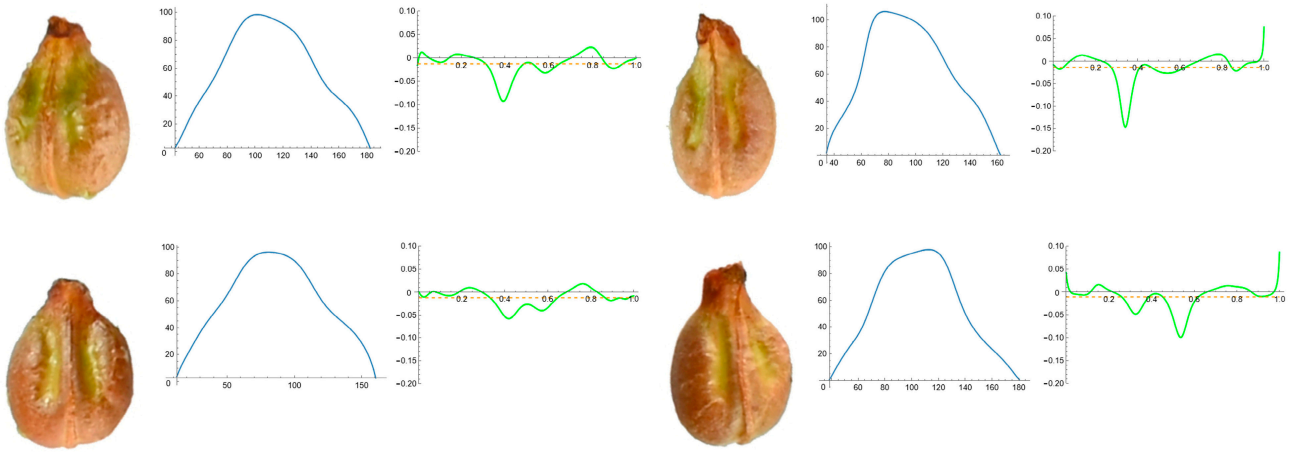

Figure 7. Four representative seeds of *Vitis riparia* with their respective Bézier curves representing their apex and the corresponding curvature values. Bar represents 5 mm. Solid lines in blue: Bézier curve. Solid lines in green: curvature. Dashed lines: mean curvature.

3.5. Symmetry Analysis

The results of symmetry quantification in nine species of *Vitis* and three related species are presented in Table 5. The highest values of symmetry were found in *P. quinquefolia*, and the lowest were found in *V. labrusca*. Among the *Vitis* species, significant differences were found between *V. labrusca* and all the other species, as well as between *V. rupestris* (with higher values) and *V. aestivalis* and *V. amurensis* (with lower values).

Table 5. Percent of symmetry in nine species of *Vitis* and three related species (coefficients of variation between parentheses). Different super index letters indicate significant differences between means for the same measurement (same column).

Species	Symmetry
Ampelopsis aconitifolia Bunge	92.28 ^{cde} (2.1)
Cissus verticillata (L.) Nicolson and C.E. Jarvis	91.23 ^{bcd} (1.6)
Parthenocissus quinquefolia (L.) Planch.	92.40 ^{e} (1.8)
Vitis aestivalis Michx.	90.85 ^{b} (1.6)
Vitis amurensis Rupr.	91.25 ^{bc} (0.8)
Vitis berlandieri Planch.	91.70 ^{bcde} (1.7)
Vitis californica Parry	92.13 ^{bcde} (1.9)
Vitis candicans Engelm. ex A.Gray	91.33 ^{bcd} (1.3)
Vitis doaniana Munson ex Viala	90.99 ^{bcde} (3.0)
Vitis labrusca L.	88.57 ^{a} (2.6)
Vitis riparia A. Gray	91.53 ^{bcde} (1.6)
Vitis rupestris Scheele	92.51 ^{de} (1.4)

4. Discussion

Seeds within the Vitaceae family exhibit a diverse range of shapes, often featuring protrusions of varying sizes and shapes on their surfaces across different genera [38]. In genera such as *Vitis* and its relatives, seeds typically possess a slightly compressed, rounded shape with a discernible polarity in length. This polarity distinguishes an apical side, where they attach to the berry pedicel, from a free basal side, which tends to be more rounded. Variable bilateral symmetry is observed along the major axis, while in the third dimension (height), the dorsal side tends to be more rounded compared to the ventral side, which may contain a rib. Consequently, seeds may exhibit characteristic forms, ranging from a water drop to a heart shape [24,25,38].

An often-overlooked aspect in seed shape analysis is the stability of shape within populations, whether within defined populations at specific stages or across populations of the same species grown under different geographical or climatic conditions. Low *J* index values for seeds within a population, when tested against the average silhouette of the same population, indicate significant shape variation. This phenomenon was observed in populations of *V. californica* and *V. aestivalis* in this study, with respective *J* index values of 86.5 and 87.5, and, to a lesser extent, in *V. riparia*, *V. rupestris* and *V. labrusca* (88.1, 88.3, and 88.6 respectively). High coefficients of variation for general morphological measurements in these populations further support the notion of shape variation. Other populations corresponding to different species exhibited *J* index values close to or over 90, indicating shape homogeneity within those populations. Another significant aspect concerns the similarity of seed shapes between different populations of the same species. For instance, seed images of *V. aestivalis* shown on the University of Michigan website [39] are different from those in our study (see later). Similarly, the seeds of *V. labrusca* in Ardeghi et al. [40] are also slightly different than those here and in our previous work [24]. It remains to be investigated whether these variations are due to environmental factors and the extent of shape variation between populations of each species. Considering the scarcity of recent morphological studies compared to molecular analyses, further research is warranted to enhance our understanding of shape variation in seed populations.

The results of shape comparison with models derived from average silhouettes have been expressed in terms of *J* index, representing the percentage of similarity between seed images and the average silhouette of each species. These relationships were visualized in a dendrogram. Phylogenetic dendrograms of *Vitis* and related species have been elaborated using various DNA sequence-based methods, generally indicating clear separation between genera such as *Cissus*, *Ampelopsis* and *Parthenocissus* from *Vitis* species [41–44]. In our dendrogram, the species of different genera, *Ampelopsis aconitifolia*, *Cissus verticillata*, and *Parthenocissus quinquefolia*, were dispersed among the species of *Vitis*. From the point

of view of shape analysis, it may be interesting to note the increased similarity with *Ampelopsis*, *Cissus* or *Parthenocissus* in the different species of *Vitis*, as was recently observed in Cucurbitaceae [26]. However, as observed in Cucurbitaceae, these results underscore the limitations of using the *J* index with geometric models in taxonomy beyond the genus level. The application of seed shape analysis to taxonomic categories higher than genera results in a high degree of homoplasy, where a parallel evolution of a given character in different groups does not necessarily reflect a phylogenetic relationship [45]. Nevertheless, the dendrogram based on the *J* index was very similar to the dendrogram resulting from the analysis performed using data from the general measurements, as well as curvature and symmetry analysis, indicating the applicability of *J* index as a general measurement for taxonomic purposes at the infra-generic level. Additionally, our results align with the relationship between *Vitis* species observed in dendrograms based on molecular analysis, particularly the associations between *V. riparia* and *V. berlandieri*, as well as between *V. amurensis* and *V. doaniana* [43].

In the dendrogram, species of *Vitis* could be grouped into two distinct clusters. One included *V. rupestris*, *V. californica* and *V. candicans*, associated to *Ampelopsis aconitifolia*, and the other was formed from the remaining species, associated with *Cissus verticillata*. The first group (associated with *Ampelopsis*) had, in general, lower curvature values, while species with higher curvature values (*V. berlandieri*, *V. amurensis*, *V. doaniana*, *V. labrusca*, *V. riparia*) were found in the second group. The species with the highest value of aspect ratio, *V. aestivalis*, gave lowest values of *J* index when compared to other species. In consequence, this species was clearly divergent in the dendrogram based on all *J* index values.

An intriguing aspect is the comparison of seed morphology between *Vitis* species and varieties and cultivars of *V. vinifera*. Most species described here displayed low aspect ratios between 1.28 and 1.5 (Stummer index between 0.74 and 0.78). In archeobotany, the seeds found with these values are sometimes described as *V. sylvestris* [17], and in fact, their average silhouettes resemble the model described for this species [25]. On the other hand, lower values of Stummer index are attributed to cultivated *V. vinifera* varieties. However, the values observed for *V. aestivalis* seeds in this study, corresponding to a Stummer index of 0.54, indicate elongated seeds in some species other than *V. vinifera*, at least under cultivation. Nevertheless, this finding contradicts data from other sources [39,43], where *V. aestivalis* seeds had a higher Stummer index, and must be interpreted with caution, until the results of further analysis with other populations of *V. aestivalis* are available.

It is widely accepted that most European *Vitis* cultivars originated from the domestication of *V. vinifera* ssp. *sylvestris* (C.C.Gmel.) Hegi (wild grape) [46–48]. Nevertheless, the possibility that some cultivated varieties had their origin in other species remains open as a subject of further investigation. Among the species assessed in this work, *V. aestivalis*, *V. berlandieri*, *V. labrusca*, and *V. rupestris* have already been recognized as allochthonous and naturalized in Europe [49]. The adscription of a given shape to a *Vitis* species, variety or form requires the analysis of many seeds with multiple origins and diverse growth conditions.

5. Conclusions

The comparative analysis of seed shapes across genera within different tribes of the Vitaceae family indicates a high degree of homoplasy in this family that probably prevents taxonomic application in categories higher than genus. Nevertheless, within the same genus, there can be a quantitative application, as demonstrated here in the case of *Vitis*. As *Vitis* is a genus with species both wild and domesticated in the Mediterranean area, with hard seeds and frequently found in archeological sites, the use of seed morphological methods based on shape quantification and comparison is a promising technique in paleobotany and archeology, as well as for the phenotyping of varieties. The protocols developed here contribute to establishing relationships between *Vitis* species and varieties, and allow us to check hypotheses, such as whether the origin of the cultivated varieties was within *V. vinifera* var. *sylvestris*, as is currently accepted, or whether other species of *Vitis* may be at the origin of some cultivars.

Supplementary Materials: The following are available at Zenodo (https://zenodo.org/uploads/10628169; accessed on 18 February 2024): (1) Seed images of all species analyzed (JPEG, color, used in curvature analysis; JPEG, black and white, used for general morphological measurements, symmetry and *J* index calculation). (2) Images used for *J* index calculation. (3) Images used for symmetry analysis. (4) Mathematica files for curvature analysis. The protocol to derive average silhouettes is described in: https://zenodo.org/record/4478344#.YBPOguhKiM8; accessed on 18 February 2024.

Author Contributions: Conceptualization, E.C.; methodology, J.J.M.-G., J.L.R.-L., D.G.d.P., F.C.S.d.S., G.M.-O., Á.T. and E.C.; software, J.J.M.-G.; validation, J.J.M.-G., J.L.R.-L., D.G.d.P., F.C.S.d.S., G.M.-O., Á.T. and E.C. formal analysis, J.J.M.-G., J.L.R.-L., F.C.S.d.S., G.M.-O., Á.T. and E.C.; investigation, J.J.M.-G., J.L.R.-L., D.G.d.P., F.C.S.d.S., G.M.-O., Á.T. and E.C.; resources, J.J.M.-G., J.L.R.-L., D.G.d.P., F.C.S.d.S., G.M.-O., Á.T. and E.C.; data curation, J.J.M.-G.; writing—original draft preparation, E.C.; writing—review and editing, J.J.M.-G., J.L.R.-L., D.G.d.P., F.C.S.d.S., G.M.-O., Á.T. and E.C. All authors have read and agreed to the published version of the manuscript.

Funding: Project "CLU-2019-05-IRNASA/CSIC Unit of Excellence", funded by the Junta de Castilla y León and co-financed by the European Union (ERDF "Europe drives our growth").

Institutional Review Board Statement: Not applicable.

Informed Consent Statement: Not applicable.

Data Availability Statement: The original contributions presented in the study are included in the article and Supplementary Material, further inquiries can be directed to the corresponding author.

Conflicts of Interest: The authors declare no conflicts of interest.

Appendix A

Figures A1–A5. Curvature analysis in seeds representative of the acute type (one point of maximum curvature). Figures A1–A5 contain four representative seeds of *C. verticillata*, *P. quinquefolia*, *V. amurensis*, *V. doaniana* and *V. labrusca*, respectively, with the Bézier curves representing their apex and the corresponding curvature values.

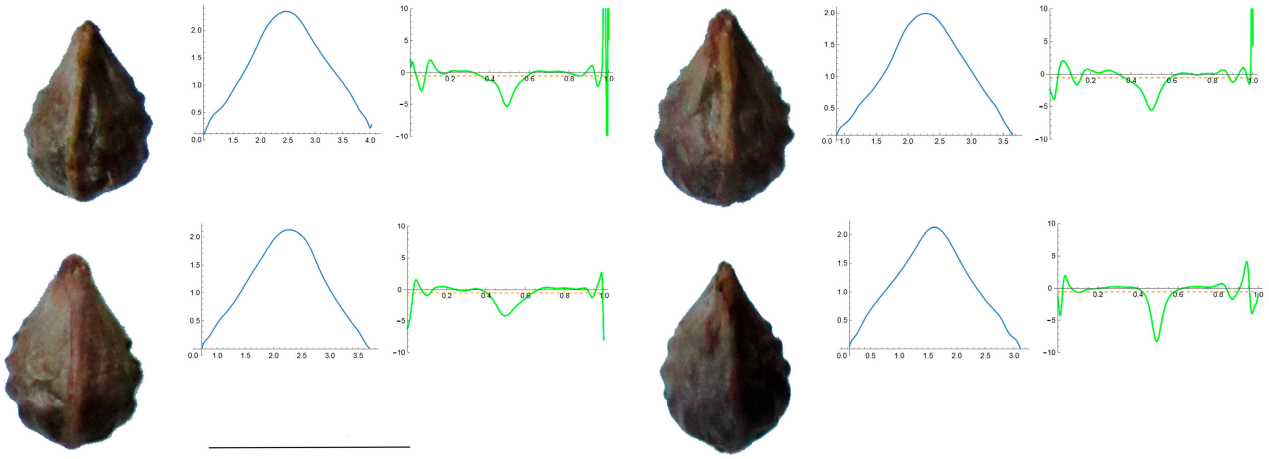

Figure A1. Four representative seeds of *Cissus verticillata* with their respective Bézier curves representing their apex and the corresponding curvature values. Bar represents 5 mm. Solid lines in blue: Bézier curve. Solid lines in green: curvature. Dashed lines: mean curvature.

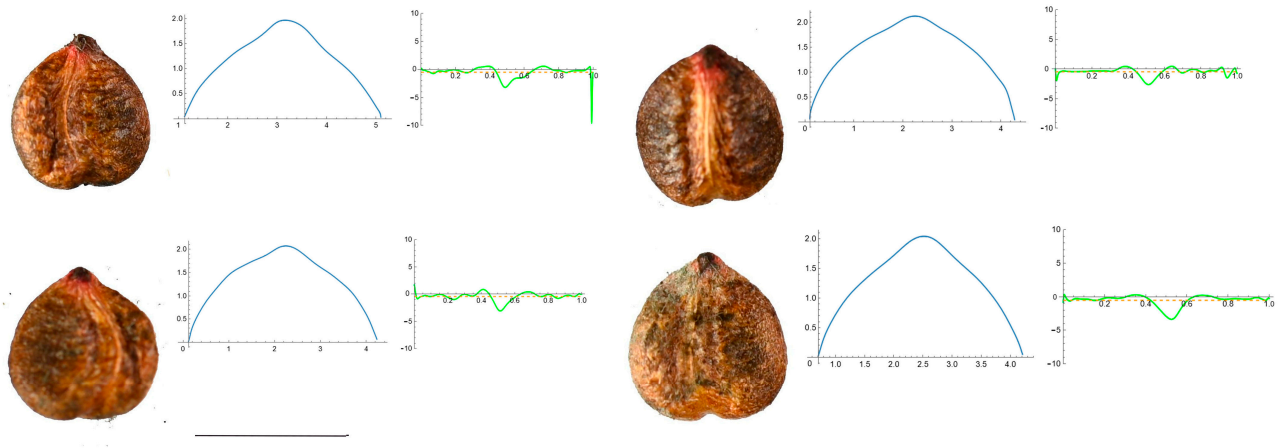

Figure A2. Four representative seeds of *Parthenocissus quinquefolia* with their respective Bézier curves representing their apex and the corresponding curvature values. Bar represents 5 mm. Solid lines in blue: Bézier curve. Solid lines in green: curvature. Dashed lines: mean curvature.

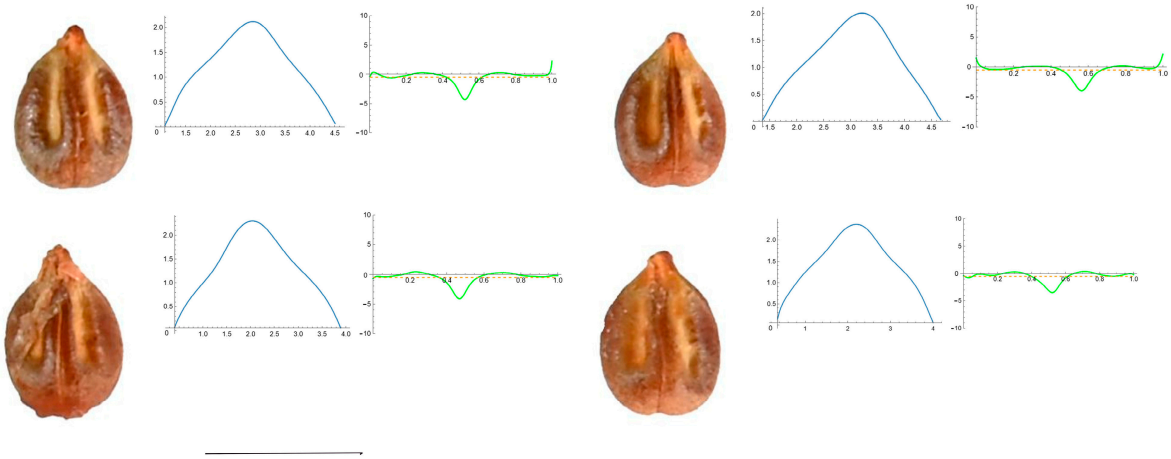

Figure A3. Four representative seeds of *Vitis amurensis* with their respective Bézier curves representing their apex and the corresponding curvature values. Bar represents 5 mm. Solid lines in blue: Bézier curve. Solid lines in green: curvature. Dashed lines: mean curvature.

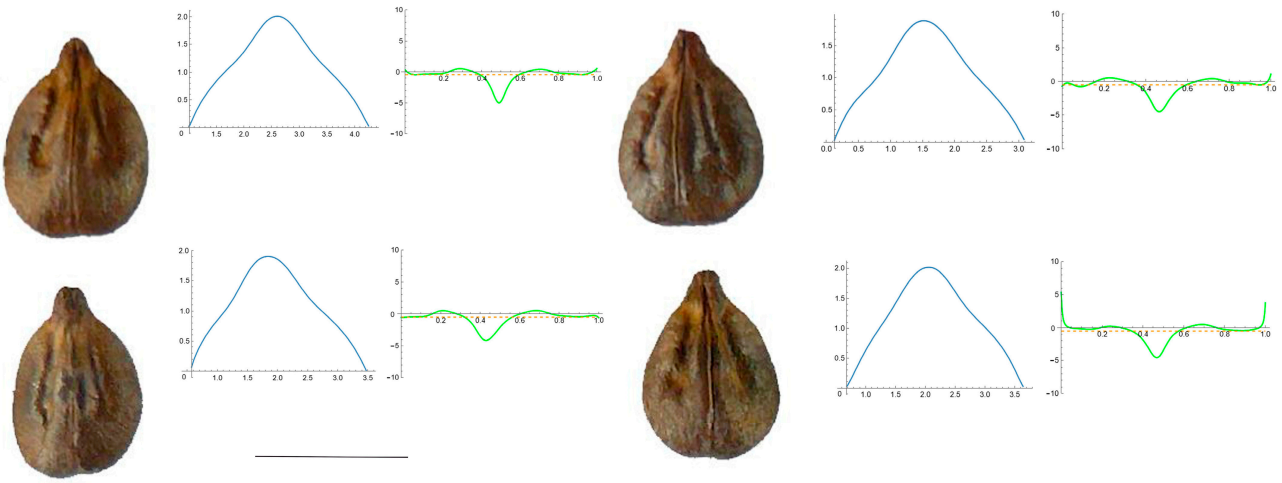

Figure A4. Four representative seeds of *Vitis* x *doaniana* with their respective Bézier curves representing their apex and the corresponding curvature values. Bar represents 5 mm. Solid lines in blue: Bézier curve. Solid lines in green: curvature. Dashed lines: mean curvature.

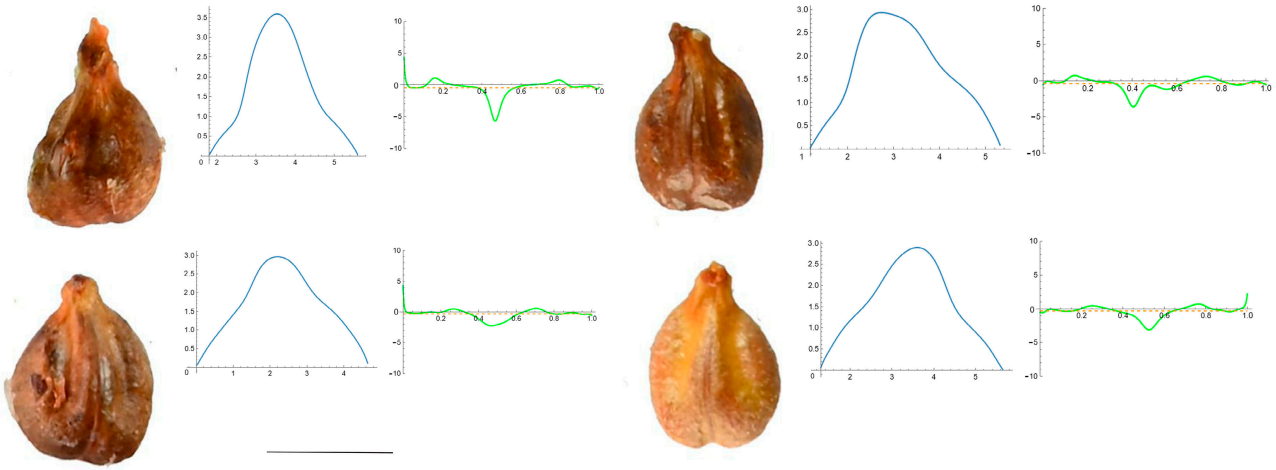

Figure A5. Four representative seeds of *Vitis labrusca* with their respective Bézier curves representing their apex and the corresponding curvature values. Bar represents 5 mm. Solid lines in blue: Bézier curve. Solid lines in green: curvature. Dashed lines: mean curvature.

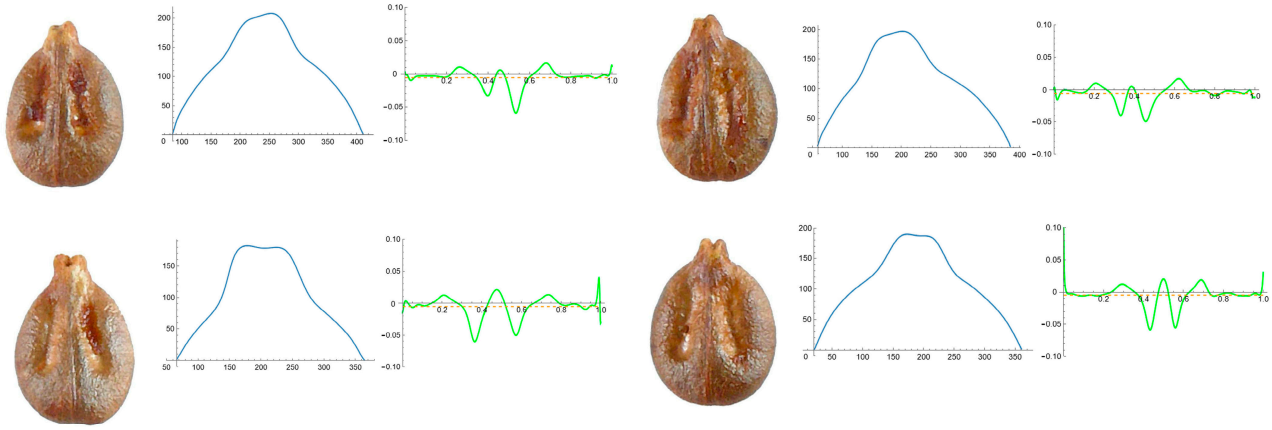

Figure A6. Four representative seeds of *Vitis berlandieri* with their respective Bézier curves representing their apex and the corresponding curvature values. Bar represents 5 mm. Solid lines in blue: Bézier curve. Solid lines in green: curvature. Dashed lines: mean curvature.

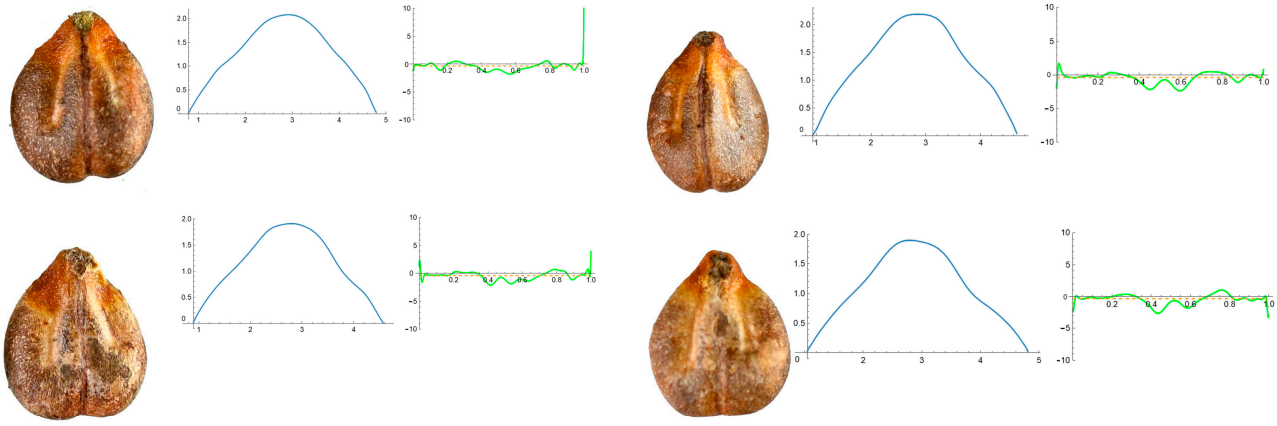

Figure A7. Four representative seeds of *Vitis candicans* with their respective Bézier curves representing their apex and the corresponding curvature values. Bar represents 5 mm. Solid lines in blue: Bézier curve. Solid lines in green: curvature. Dashed lines: mean curvature.

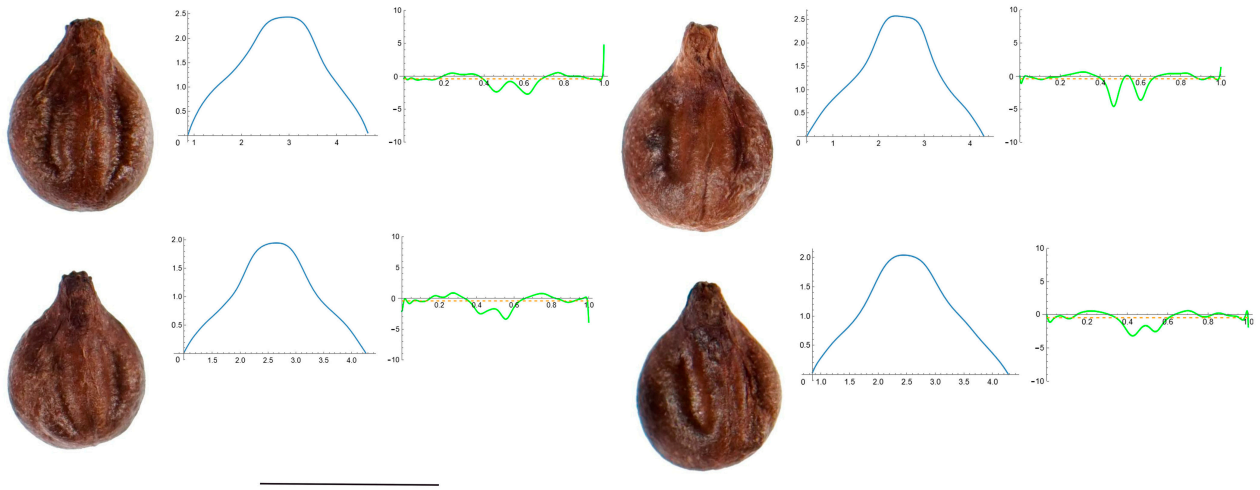

Figure A8. Four representative seeds of *Vitis rupestris* with their respective Bézier curves representing their apex and the corresponding curvature values. Bar represents 5 mm. Solid lines in blue: Bézier curve. Solid lines in green: curvature. Dashed lines: mean curvature.

References

1. FAO. Food and Agriculture Organization of the United Nations. Available online: http://faostat.fao.org (accessed on 18 February 2024).
2. OIV. Office International de la Vigne et du Vin. Available online: http://www.oiv.int/ (accessed on 18 February 2024).
3. Vivier, M.A.; Pretorius, I.S. Genetically tailored grapevines for the wine industry. *Trends Biotechnol.* **2002**, *20*, 472–478. [CrossRef]
4. Wen, J. Vitaceae. In *The Families and Genera of Vascular Plants*; Kubitzki, K., Ed.; Springer: Berlin/Heidelberg, Germany, 2007; Volume 9, pp. 467–479.
5. POWO. Plants of the World Online. Facilitated by the Royal Botanic Gardens, Kew. Published on the Internet. 2023. Available online: http://www.plantsoftheworldonline.org/ (accessed on 18 February 2024).
6. Arrigo, N.; Arnold, C. Naturalised *Vitis* Rootstocks in Europe and consequences to native wild grapevine. *PLoS ONE* **2007**, *2*, e521. [CrossRef]
7. Pipia, I.; Gogniashvili, M.; Tabidze, V.; Beridze, T.; Gamkrelidze, M.; Gotsiridze, V.; Melyan, G.; Musayev, M.; Salimov, V.; Beck, J.; et al. Plastid DNA sequence diversity in wild grapevine samples (*Vitis vinifera* subsp. *sylvestris*) from the Caucasus region. *Vitis* **2012**, *51*, 119–124.
8. Laguna Lumbreras, E. Sobre las formas naturalizadas de *Vitis* L. (Vitaceae) en la Comunidad Valenciana, I. Especies. *Flora Montiberica* **2003**, *23*, 46–82.
9. Jacquat, C.H.; Martinoli, D. *Vitis vinifera* L.: Wild or cultivated? Study of the grape pips found at Petra, Jordan; 150 B.C.-A.D. 40. *Veget. Hist. Archaeobot.* **1999**, *8*, 25–30. [CrossRef]
10. Gitea, M.A.; Bungau, S.G.; Gitea, D.; Pasca, B.M.; Purza, A.L.; Radu, A. Evaluation of the phytochemistry-therapeutic activity relationship for grape seeds Oil. *Life* **2023**, *13*, 178. [CrossRef]
11. Barbagallo, M.G.; Patti, D.; Pisciotta, A. Phenotypic traits of berries and seeds of Sicilian grape cultivars (*Vitis vinifera* L.). *Sci. Hortic.* **2020**, *261*, 109006. [CrossRef]
12. Sharafan, M.; Malinowska, M.A.; Kubicz, M.; Kubica, P.; Gémin, M.; Abdallah, C.; Ferrier, M.; Hano, C.; Giglioli-Guivarc'h, N.; Sikora, E.; et al. Shoot Cultures of *Vitis vinifera* (Vine Grape) Different cultivars as a promising innovative cosmetic raw material—Phytochemical profiling, antioxidant potential, and whitening activity. *Molecules* **2023**, *28*, 6868. [CrossRef]
13. Rivera, D.; Miralles, B.; Obón, C.; Carreño, E.; Palazón, J.A. Multivariate analysis of Vitis subgenus *Vitis* seed morphology. *Vitis* **2007**, *46*, 158–167.
14. Planchon, J.E. Ampelideae, Monographie des Ampélidées Vraies. In *Monographiae Phanerogamarum*; De Candolle, A.P., Ed.; Treuttel et Würtz: Paris, France, 1887; Volume 5, pp. 305–368.
15. Viala, P.; Péchoutre, P. *Morphologie externe de la graine In Ampélographie*; Viala, P., Vermorel, V., Eds.; Masson et Cie.: Paris, France, 1910; pp. 156–166.
16. Ocete, R.; Cantos, M.; López, M.A.; Gallardo, A.; Pérez, M.A.; Troncoso, A.; Lara, M.; Failla, O.; Ferragut, F.J.; Liñán, J. *Caracterización y Conservación del Recurso Fitogenético vid Silvestre en Andalucía*; Consejería de Medio Ambiente, Junta de Andalucía: Seville, Spain, 2007.
17. Hajnalová, M.; Látková, M.; Kajanová, M.; Eliáš jun, P.; Ďurišová, Ľ. Wild or cultivated? A study of *Vitis sylvestris* in natura in Slovakia and implications for archaeology and archaeobotany (morphometric approach). *Veg. Hist. Archaeobotany* **2023**, *32*, 321–337. [CrossRef]
18. Orrú, M.; Grillo, O.; Lovicu, G.; Venora, G.; Bacchetta, G. Morphological characterisation of *Vitis vinifera* L. seeds by image analysis and comparison with archaeological remains. *Veget. Hist. Archaeobot.* **2012**, *22*, 231–242. [CrossRef]

19. Orrú, M.; Grillo, O.; Venora, G.; Bacchetta, G. Seed morpho-colorimetric analysis by computer vision: A helpful tool to identify grapevine (*Vitis vinifera* L.) cultivars. *Grape Wine Res.* **2015**, *21*, 508–519. [CrossRef]
20. Sonka, M.; Hlavac, V.; Boyle, R. *Image Processing Analysis and Machine Vision*, 3rd ed.; Thomson Learning: Toronto, ON, Canada, 2008; 829p.
21. Ucchesu, M.; Orrú, M.; Grillo, O.; Venora, G.; Usai, A.; Serreli, P.F.; Bacchetta, G. Earliest evidence of a primitive cultivar of *Vitis vinifera* L. during the Bronze Age in Sardinia (Italy). *Veget. Hist. Archaeobot.* **2015**, *24*, 587–600. [CrossRef]
22. Ucchesu, M.; Orrú, M.; Grillo, O.; Venora, G.; Paglietti, G.; Ardu, A.; Bacchetta, G. Predictive Method for Correct Identification of Archaeological Charred Grape Seeds: Support for Advances in Knowledge of Grape Domestication Process. *PLoS ONE* **2016**, *11*, e0149814. [CrossRef]
23. Milanesi, C.; Costantini, L.; Firmati, M.; Antonucci, F.; Faleri, C.; Buracchi, A.; Cresti, M. Geometric morphometry and archaeobotany: Characterisation of grape seeds (*Vitis vinifera* L.) by analysis of form. *Open Access Libr. J.* **2014**, *1*, e634. [CrossRef]
24. Martín-Gómez, J.J.; Gutiérrez del Pozo, D.; Ucchesu, M.; Bacchetta, G.; Cabello Sáenz de Santamaría, F.; Tocino, Á.; Cervantes, E. Seed morphology in the Vitaceae based on geometric models. *Agronomy* **2020**, *10*, 739. [CrossRef]
25. Cervantes, E.; Martín-Gómez, J.J.; Espinosa-Roldán, F.E.; Muñoz-Organero, G.; Tocino, Á.; Cabello-Sáenz de Santamaría, F. Seed morphology in key Spanish grapevine cultivars. *Agronomy* **2021**, *11*, 734. [CrossRef]
26. Martín-Gómez, J.J.; Gutiérrez del Pozo, D.; Rodríguez-Lorenzo, J.L.; Tocino, Á.; Cervantes, E. Geometric analysis of seed shape diversity in the Cucurbitaceae. *Seeds* **2023**, *3*, 40–55. [CrossRef]
27. Cervantes, E.; Tocino, A. Geometric analysis of Arabidopsis root apex reveals a new aspect of the ethylene signal transduction pathway in development. *J. Plant Physiol.* **2005**, *162*, 1038–1045. [CrossRef]
28. Noriega, A.; Tocino, A.; Cervantes, E. Hydrogen peroxide treatment results in reduced curvature values in the Arabidopsis root apex. *J. Plant Physiol.* **2009**, *166*, 554–558. [CrossRef]
29. Martín-Gómez; Rewicz; Goriewa-Duba; Wiwart; Tocino; Cervantes Morphological Description and classification of wheat kernels based on geometric models. *Agronomy* **2019**, *9*, 399. [CrossRef]
30. Cervantes, E.; Martín-Gómez, J.J.; Espinosa-Roldán, F.E.; Muñoz-Organero, G.; Tocino, Á.; Cabello Sáenz de Santamaría, F. Seed apex curvature in key Spanish grapevine cultivars. *Vitic. Data J.* **2021**, *3*, e66478. [CrossRef]
31. Wen, J.; Lu, L.-M.; Nie, Z.-L.; Liu, X.-Q.; Zhang, N.; Ickert-Bond, S.; Gerrath, J.; Manchester, S.R.; Boggan, J.; Chen, Z.-D. A new phylogenetic tribal classification of the grape family (Vitaceae). *J. Syst. Evol.* **2018**, *56*, 262–272. [CrossRef]
32. Ferreira, T.; Rasband, W. Imagej User Guide-Ij1.46r. 2012; 186 p. Available online: http://imagej.nih.gov/ij/docs/guide (accessed on 19 May 2020).
33. Cox, E.P. A method of assigning numerical and percentage values to the degree of roundness of sand grains. *J. Paleontol.* **1927**, *1*, 179–183.
34. Riley, N.A. Projection sphericity. *J. Sediment. Pet.* **1941**, *11*, 94–97.
35. Schwartz, H. Two-dimensional feature-shape indexes. *Mikroskopie* **1980**, *37*, 64–67.
36. Sokal, R.R.; Braumann, C.A. Significance tests for coefficients of variation and variability profiles. *Syst. Zool.* **1980**, *29*, 50. [CrossRef]
37. Martín-Gómez, J.J.; Rodríguez-Lorenzo, J.L.; Tocino, Á.; Janoušek, B.; Juan, A.; Cervantes, E. The outline of seed silhouettes: A morphological approach to *Silene* (Caryophyllaceae). *Plants* **2022**, *11*, 3383. [CrossRef] [PubMed]
38. Cervantes, E.; Martín-Gómez, J.J.; Gutiérrez del Pozo, D.; Tocino, Á. Seed Geometry in the Vitaceae. *Plants* **2021**, *10*, 1695. [CrossRef]
39. Burnham, R.J. Climbers. Censusing Lianas in Mesic Biomes of Eastern Regions. *Vitis aestivalis* Michx. Available online: https://climbers.lsa.umich.edu/vitis-aestivalis/ (accessed on 18 February 2024).
40. Ardenghi, N.M.G.; Galasso, G.; Banfi, E.; Cauzzi, P. *Vitis* × *novae-angliae* (Vitaceae): Systematics, distribution and history of an "illegal" alien grape in Europe. *Willdenowia* **2015**, *45*, 197–207. [CrossRef]
41. Wan, Y.; Schwaninger, H.R.; Baldo, A.M.; Labate, J.A.; Zhong, G.Y.; Simon, C.J. A phylogenetic analysis of the grape genus (*Vitis* L.) reveals broad reticulation and concurrent diversification during neogene and quaternary climate change. *BMC Evol. Biol.* **2013**, *13*, 141. [CrossRef] [PubMed]
42. da Costa, A.F.; Teodoro, P.E.; Bhering, L.L.; Tardin, F.D.; Daher, R.F.; Campos, W.F.; Viana, A.P.; Pereira, M.G. Molecular analysis of genetic diversity among vine accessions using DNA markers. *Genet. Mol. Res.* **2017**, *16*, gmr16029586. [CrossRef]
43. Péros, J.P.; Launay, A.; Peyrière, A.; Berger, G.; Roux, C.; Lacombe, T.; Boursiquot, J.M. Species relationships within the genus *Vitis* based on molecular and morphological data. *PLoS ONE* **2023**, *18*, e0283324. [CrossRef]
44. Kerekes, A.; Tóth-Lencsés, K.A.; Kiss, E.; Szőke, A. Phylogeny of *Vitis* species based on a VvMybA1 marker analysis. *Acta Hortic.* **2019**, *1248*, 135–140. [CrossRef]
45. Hall, B.K. Homology and homoplasy. In *Handbook of the Philosophy of Science, Philosophy of Biology*; Matthen, M., Stephens, C., Eds.; Elsevier: Amstercam, The Netherlands, 2007; pp. 429–453.
46. Olmo, H. The origin and domestication of the Vinifera grape. In *The Origins and Ancient History of Wine*; McGovern, P.E., Fleming, S.J., Katz, S.H., Eds.; Gordon and Breach: Amsterdam, The Netherlands, 1995; pp. 31–43.
47. Cunha, J.; Baleiras-Couto, M.; Cunha, J.P.; Banza, J.; Soveral, A.; Carneiro, L.C.; Eiras-Dias, J.E. Characterization of Portuguese populations of *Vitis vinifera* L. ssp. sylvestris (Gmelin) Hegi. *Genet. Resour. Crop. Evol.* **2007**, *54*, 981–988. [CrossRef]

48. Arroyo-García, R.; Lefort, F.; De Andrés, M.; Ibáñez, J.; Borrego, J.; Cabello, F.; Martínez-Zapater, J.M. Haplotypic polymorphisms for chloroplast microsatellites analysis in *Vitis*. *Genome* **2002**, *45*, 1142–1149. [CrossRef] [PubMed]
49. Webb, D.A. Vitis. In *Flora Europaea 2*; Tutin, T.G., Heywood, V.H., Burges, N.A., Moore, D.M., Valentine, D.M., Walters, S.M., Webb, D.A., Eds.; Cambridge University Press: Cambridge, UK, 1968; Volume 246.